



RFO-MNN: MODULAR NEURAL NETWORK OPTIMIZED WITH RED FOX OPTIMIZATION FOR SPECKLE NOISE SUPPRESSION IN ULTRASOUNDIMAGES

G. Karthiga^{1*}, S. Allwin¹

Abstract

Diagnostic and therapeutic procedures such as intraarticular injections and biopsy can be guided using ultrasound imaging in the treatment of joint arthropathies. This paper has concentrated on ultrasound images more explicitly, on the concealment techniques for the multiplicative noise. This work has contrasted with various denoising techniques used to suppress the SN in medicinal images acquired through ultrasound images. The de-speckling approach has been done in two phases; A bilateral filter (BF) is employed in the first step to reduce the speckle noise. The modular neural network (MNN) is trained using statistical features has been utilized to suppress the SN in US images. MNN was optimized with red fox optimization (RFO) algorithm for normalize the output. The simulation outcomes demonstrate that the BF based RFO-MNN filtering method performs better for the multiplicative noise concealment in US images. The better quality of denoised images is observed by using BF based RFO-MNN over other methods such that DTCWT-IBTV, BF and ANN. The proposed method BF based RFO-MNN produced better quality of de-speckled images with the PSNR of 34.89, SSIM of 0.89 and EPI of 0.67 values for ultrasound images.

Key Words: Ultrasound images, speckle noise, Modular neural network (MNN), Red fox optimization (RFO) algorithm, Bilateral filter (BF).

DOI Number: 10.14704/nq.2022.20.6.NQ22188

NeuroQuantology2022; 20(6):1890-1897

1890

Introduction

Clinical imaging is the procedure for producing visual representations of the interior of the body for clinical assessment and surgical treatment, as well as visual images of the function of specific organs or tissues [1]. Radiography is still the most commonly used medical imaging system in the evaluation of knee osteoarthritis in modern imaging modalities. In general, the knee joint is evaluated using an extended-knee radiograph, which is a bilateral anterior-posterior image

obtained with weight-bearing patients with both knees fully extended. X-ray imaging has typically used film to capture the images [2]. The images are formed as a result of X-ray absorption by body structures. Non-absorbed X-rays pass through the body and strike a film behind the area of the body. The light- and radiation-sensitive film is sandwiched between two intensifying screens, which are housed in a lightproof cassette [3]. The X-ray radiation is converted into light by the screens, which then acts on the film.

*** Corresponding Author:** G. Karthiga.

Address: ¹Department of CSC, Infant Jesus College of Engineering, Anna University, Tuticorin, 628251, India

E-mail: karthigapapers@gmail.com

Ultrasound is widely used to provide imaging guidance for procedures such as intra-articular injection and biopsy in the diagnosis and treatment of joint arthropathies. Thus, even in the absence of other clinical data, US is useful for detecting early osteoarthritis [4,5]. The probe intensity will vary

depending on the structure, but it will be between 7 and 10MHz in general, with the upper end providing finer detail [14]. Even higher frequencies, around 13 MHz, will aid in the creation of a "soft image" with a high level of detail. The US image is created by the reflection of waves of body structures. It may be a sound wave with



frequencies higher than the upper capable of being heard restrain of human hearing. Ultrasound devices work with frequencies from 20 kHz to a few gigahertz [15]. An US images are affected with speckle noise (SN) while procurement, transmission and retrieval process. Clatter which in US-images could be categorized as, salt and pepper, Gaussian, and SN noise. Speckle could be a specific type of noise which happens in US images gotten by articulate imaging schemes like US [16]. It is induced by obstructions amid similar waves that, reflected from common exteriors, attain out of stage in sensor [17].

A neural network (NN) method is considered to categorize SN into three wide measurable groups, and it has been utilized effectively both in likelihood thickness estimation and for filtering of multiplicative noise in US images [18, 19]. It is also expected that; every dissemination could be described by constraints. Different characteristics are calculated from whole speckle noisy images and are in this way utilized as input to multilayer neural systems with ceaseless output values [20]. The systems recognize parameters in two covering stages: (1) Evaluation of the parameter of speckle noise and (2) Removal of speckle noise. NN have a long history of victory in classification issues, counting infection description in ultrasound scans. It has been appeared to be all-inclusive approximators, given an adequate number of units within the networks covered up layers.

The rest of this paper was organized as follows. Section-2 encompasses of literature survey, Section-3 includes the proposed BF based RFO-MNN filtering framework, Section-4 comprises with result and discussion and finally Section-5 encloses with conclusion and future enhancement.

Literature survey

Ultrasound images must be of very high quality in order to serve their intended purpose. Because of the instability, noise, and incompleteness of the data, pre-processing is critical in imaging. Many methods for creating ultrasound images in various ways have been developed and implemented and some of the researches are briefly discussed in this section.

Noise categorization is determined by the origin and induce of the noise. According to [6], noise is divided into two types: blur noise, such as Gaussian noise, and impulse noise, like salt and pepper. On

the one hand, blur noise is dispersed in equal proportions throughout the image. It changes the values of all pixels either upwards or downwards. It is referred to as blur motion if it is moved in a specific direction. The first stage in medical image processing methods is de-noising. Various algorithms and filters have been developed to improve degraded images while retaining their key aspects [7]. The interpreter can specify in images and accomplish quick and accurate visual assessments to image de-noising. Image de-noising algorithms are widely used in the medical image field with great success. The most widely used nonlinear filter is the median filter. It compensates for impulsive noise while preserving edge information [8]. Nonlinear filtering includes diffusion filtering. It includes Anisotropic Diffusion (AD) filters for removing noise from images.

Wavelet algorithms are well-known as novel approaches to image processing problems [9]. We can use Wavelet algorithms to remove noise from images by converting them to the wavelet domain. It is critical in wavelet transform to choose a function with a time-domain integral of zero. Feature extraction is a type of dimensionality reduction that is unique. It is carried out after the pre-processing stages in image processing methodology by isolating the unnecessary traits from the relevant ones. The reduction in features allows you to select the aspects that are best suited for categorization based on various criteria. It employs a classifier to identify the desired characteristics [10]. We can use Wavelet algorithms to remove noise from images by converting them to the wavelet domain. It is critical in wavelet transform to choose a function with a time-domain integral of zero. When compared to traditional Fourier analysis, the wavelet transform can analyse functions in both the spatial and time domains [11]. The application could be based on characteristics, and local features could be attained via edge detection or by using local statistical data such as standard deviation and mean. Wavelets were used in a wide variety of applications including signal processing, data reduction, levelling, and image de-noising [12]. The Wiener filter's goal is to reduce the amount of noise in a signal by comparing it to an estimate of the desired noise - free signal. It uses a statistical method to eliminate noise from a signal and is regarded as outstanding for de - noising or image de-blurring. The Wiener filter [13] process requires information on the noise and original signal spectra, and its



model complexity control relates to the window size.

In the literature, the main challenge for ultrasound images is low contrast and interference from speckle noise. To overcome this challenge, we propose a filtering method and modular neural networks with red fox optimization for suppression of speckle noise based on US images.

Proposed method

The block diagram of proposed Speckle suppression using BF and MNN is given in fig. 1. In this method, two stages of de-speckling process have been performed. During the first stage, BL has

been used for the filtering process. Then, the denoised image and the original ultrasound images are subtracted in order to get the filtered speckle noise. After that, the statistical characteristics such that mean, median, standard deviation and kurtosis are calculated from the filtered speckle noise image. These features are utilized to train MNN. In the second stage of filtering process, these trained MNN has been used to de-speckle the filtered image which are from the output of bilateral filter. At last, the performance metrics such that, PSNR, SSIM and EPI are evaluated so as to get the efficiency of BF based RFO-MNN filtering method.

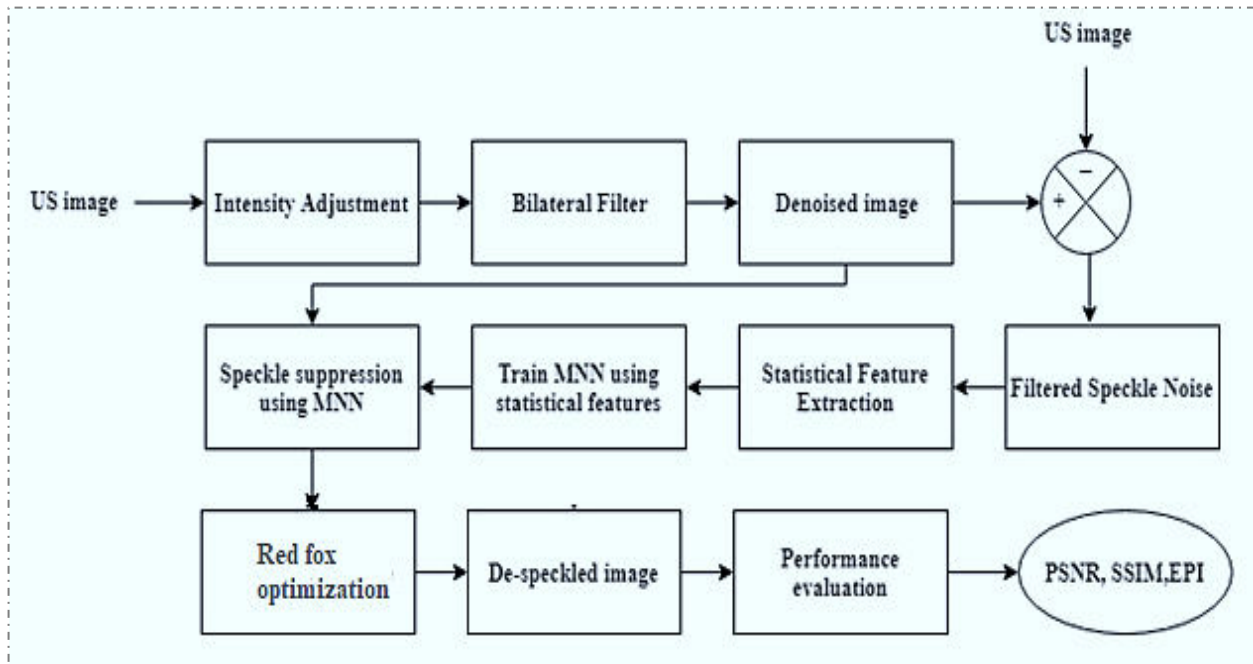


Fig.1: Block diagram of speckle suppression using BF based RFO-MNN

Intensity Adjustment

Initially, US image is given as input to the intensity adjustment block as shown in fig.4.1. Here, Histogram Equalization (HE) method has been used for intensity adjustment. HE is performed by remapping the dim degrees of an image dependent on the likelihood dissemination of the input gray levels. It straightens and extends the dynamic scope of the image histogram and bringing in overall contrast enhancement image.

Bilateral Filter

The intensity esteems at every pixel in a denoised image are supplanted by an average of pixel intensity esteems from neighboring pixels.

This weight can be founded on Gaussian distribution. Vitally the weight does not only depend on Euclidean separation but depends on the radiometric distinction. These characteristics of bilateral filter preserves the sharp edges by efficiently circling through every pixel and modifying loads to the contiguous pixels accordingly. The objective function of bilateral function is expressed as,

$$B^{Filtered} = \sum_{x_i} DW(x_i) k_r(\|DW(x_i) - DW(x)\|) k_s(\|x_i - x\|) \quad (1)$$

Where, $B^{Filtered}$ is the de-speckled image, DW is the filtered image using soft thresholding with SURE estimation, x is the co-ordinates of the current pixel



to be filtered, k_r is the kernel range and k_s is the spatial kernel function for smoothing images.

$$m = (s_m + s_{m+1})/2 \tag{5}$$

Statistical Feature Extraction

The main objective of feature extraction is to extract a set of characters, which maximizes the identification rate with the slightest number of components and to produce comparable feature set for various of instance of the same image. There are many image attributes that can be utilized for train the NN which includes first order statistics like mean, standard deviation, median and kurtosis. The features are defined as follows,

$$\mu = \frac{1}{PQ} \sum_i^P \sum_j^Q f_{i,j} \tag{2}$$

$$\sigma = \sqrt{\frac{1}{PQ} \sum_{i=1}^P \sum_{j=1}^Q (f_{i,j} - \mu)^2} \tag{3}$$

$$k = PQ \frac{\sum_{i=1}^P \sum_{j=1}^Q (f_{i,j} - \mu)^4}{(\sum_{i=1}^P \sum_{j=1}^Q (f_{i,j} - \mu)^2)^2} \tag{4}$$

Speckle Suppression using MNN

The Neural Network (NN) design comprises of three layers namely, input, intermediate and output layer. Every unit of input and intermediate layer are organized 2 measurements. One size of information is standardized estimation of intensity of an image. The highest value is taken as 1 and the lowest value is taken as -1. The input layer is taken for processing by reading the data to fit in the layer size for the corresponding input image. Each unit in the input layer of the non-linear function yields the resultant information to the hidden layer. By adding weight addition to the input data, the results are generated for the hidden and output layer. Each intensity values of input image compared with the output of NN. To minimize the error the internal conditions are altered. The back-propagation algorithm is used to fully train the NN.

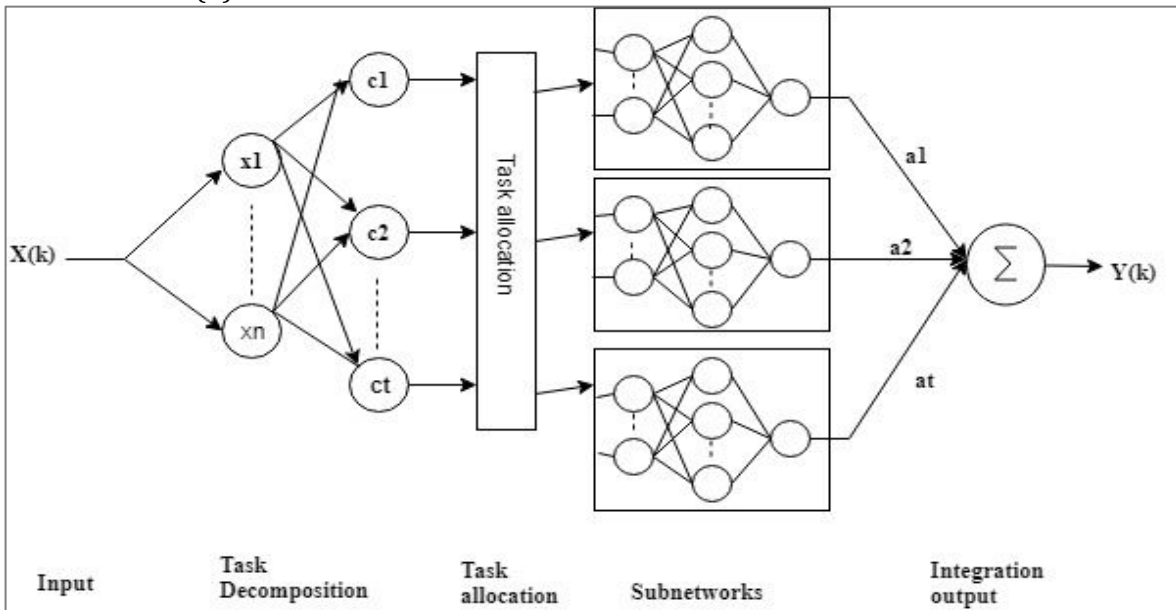


Fig.2 Structure of Modular Neural Network (MNN)

MNN system is shown in Fig.4.3. Each layer which are used in MNN are briefly explained underneath. It comprises of 'n' basis hubs, where 'n' -information factor and it is calculated as follows,

$$x(k) = [x_1(k), x_2(k), \dots, x_n(k)]^T \tag{6}$$

It comprises of a single neuron, and every neurocyte includes a kernel function which is gathered as follows,

$$k_h(x(k), c_h) = \begin{cases} 1, & |x(k) - c_h| \leq \delta_h; \\ 0, & |x(k) - c_h| > \delta_h; \end{cases} \tag{7}$$

where δ_h - ambit of the h^{th} neurocyte. This layer accepts the methodology that in case $k_h(x(k), c_h) = 1$, the h^{th} sub network made active to understand the input trial. The intermediate layer could not be implemented inside the MNN network. The input trials help to powerfully



balance the active sub network. The output is denoted in the subnetwork layer as follows,

$$y_h(k) = \sum_{i'=1}^m w_{i'}(k) f[\sum_{i=1}^n v_{ii'}(k) x_i(k)] \quad (8)$$

Where, $w_{i'}$ - weights of the intermediate and output neurocyte $v_{ii'}$ - weight of input and intermediate neurocyte in SL,

$$f(x) = \frac{1}{(1+e^{-x})} \quad (9)$$

The output of the MNN network is calculated in the integration output layer as,

$$Y(k) = \sum_{g'=1}^R \alpha_{g'}(k) y_h(k) \quad (10)$$

Where R represents no. of certain sub networks $1 \leq R \leq l$, $\alpha_{g'}(k)$ is the integration weight.

Optimization using Red fox optimization

A new metaheuristic optimization algorithm called Red Fox Optimizer (RFO) algorithm is inspired by the red fox hunting behavior. During hunting, the red fox hides behind bushes and approaches its prey slowly. It surprises its prey by attacking. RFO initialization can be modelled by random individual generation, as shown below

$$Z = \{z_0, z_1, z_2, \dots, z_{n-1}\} \quad (11)$$

where i refers to the number of populations, $(Z_j^i)^t$ describes the z_i in iteration t , and j refers to the problem dimensions in the probing space. A classifier should subsequently be used to identify diseases based on the features obtained from the feature extraction. As previously mentioned, CNN employs the backpropagation mechanism for learning. By minimizing the mean square error, this study established an RFO technique for the optimal choice of system weights in CNN. The MSE can be expressed numerically as follows:

$$mse = \frac{1}{T} \sum_{j=1}^q \sum_{i=1}^p (x_j^i - y_j^i)^2 \quad (12)$$

where p and q represent the values of the output layers and the facts, respectively, and x_j^i and y_j^i denotes the attained and the appropriate magnitudes for j^{th} unit in the network's output layer in time T respectively.

Results and discussion

US dataset has been used for this experiment. It consists of two groups namely benign and malignant. Benign consists of 100 images and malignant contains 150 images. Therefore, this US dataset totally contains 250 ultrasound images which are affected by speckle noise. In this

experiment, SN is not additionally added, because the images itself contains SN. These images are directly used for the SN reduction process.

Performance Evaluation

Performance of hybrid de-speckling method based on DTWT and improved bilateral filter can be assessed utilizing numerical proportions of image quality after the filtering method has been performed on the image. The presentation measurements are selected dependent on their processable contortion measures. MSE and PSNR are the two most well-known proportions of image quality in image processing systems (Madan Lal et al., 2016). In addition to these parameters, SSIM and EPI have also been evaluated to find the efficiency of hybrid de-speckling method. The PSNR and the MSE measures are given by (4.11) and (4.12), respectively,

$$PSNR = 10 \log \frac{(255)^2}{MSE} \quad (13)$$

$$MSE = \frac{\sum_{m=0}^{P-1} \sum_{n=0}^{Q-1} (x(m,n) - y(m,n))^2}{P \times Q} \quad (14)$$

The SSIM metric can be described as,

$$SSIM(x, y) = \frac{(2\mu_x\mu_y + C_1)(2\sigma_{xy} + C_2)}{(\mu_x^2 + \mu_y^2 + C_1)(\sigma_x^2 + \sigma_y^2 + C_2)} \quad (15)$$

Another parameter EPI can be calculated by using the equation, which is described as,

$$EPI = \frac{\sum(\Delta x - \bar{\Delta x}) \sum(\Delta y - \bar{\Delta y})}{\sqrt{\sum(\Delta x - \bar{\Delta x})^2 \sum(\Delta y - \bar{\Delta y})^2}} \quad (16)$$

Where, $x(m, n)$ - pixel esteems in the noise-free US-image, $y(m, n)$ - pixel esteems in the de-speckled image after the filtering process, P, Q are the size of the image, and $\mu_x, \mu_y, \sigma_x, \sigma_y$ and σ_{xy} are the local means, standard deviations and cross-variance respectively.

Comparative analysis

In this paper, around 30 US images have been simulated and the average values of PSNR, SSIM and EPI are calculated by using those values and tabled in table.1. From this tabulation, it can notice, the proposed methodology RFO-MNN method produces better results in terms of PSNR of 34.89, SSIM of 0.89 and EPI of 0.67. This method is compared with DTCWT-IBTV, BF and ANN methods. Here, DTCWT-IBTV method produces the



output filtered images with PSNR of 34.36, SSIM of 0.89 and EPI of 0.62. At last, the ANN produces the denoised images with the PSNR of 32.85, SSIM of 0.72 and EPI of 0.59. The BF produced de-speckled images with the PSNR of 33.83, SSIM of 0.84 and EPI of 0.59.

Table.1 Comparison of performance metrics for various de-speckling methods for benign US image

Filter Type	PSNR	SSIM	EP1
RFO-MNN	34.89	0.89	0.67
DTCWT-IBTV	34.36	0.89	0.65
BF	33.83	0.84	0.62
ANN	32.85	0.72	0.59

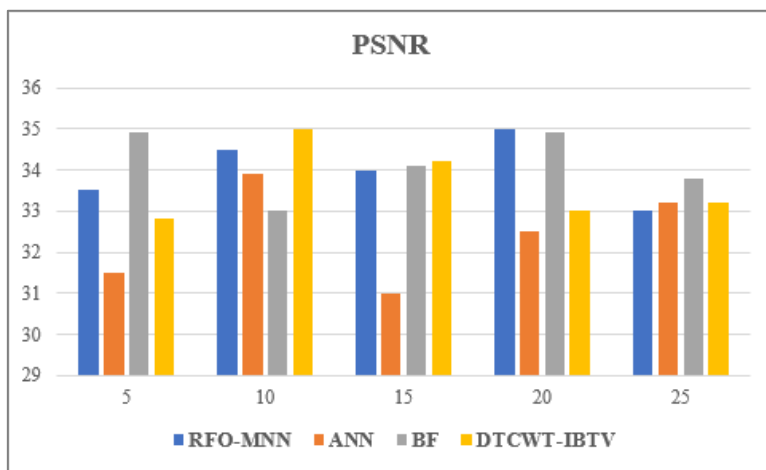


Fig.3 Graphical representation of PSNR values of performance metric for various US images

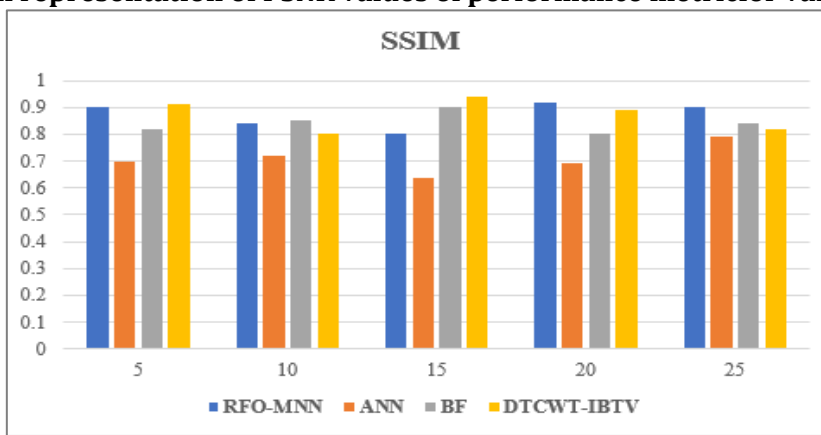


Fig.4 Graphical representation of SSIM values of performance metric for various US images



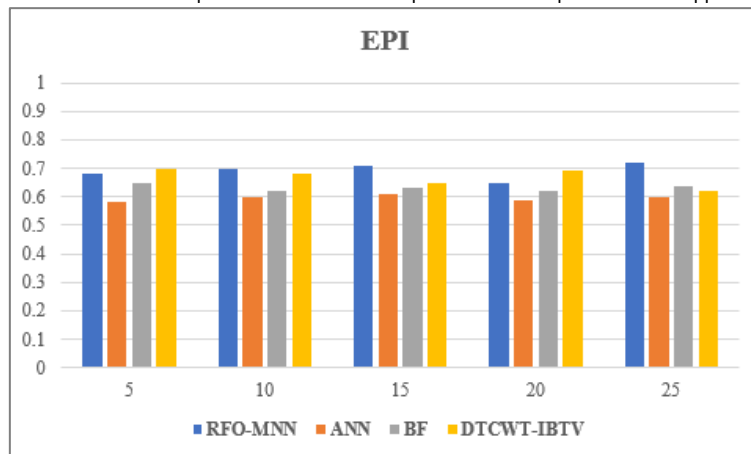


Fig.5 Graphical representation of EPI values of performance metric for various US images

The above comparison of performance metrics of various exiting methods is graphically represented in figure. 3,4 and 5. The proposed method RFO-MNN method shows improvements in terms of PSNR, SSIM and EPI over other various de-speckling methods. Therefore, RFO-MNN method is well suitable for de-speckling the various US images. In BF, some of the important attributes of original images are removed from the image. Speckle suppression using ANN produces poor segmentation results when compared with other methods. In this method, the speckle noise is not filtered properly. After visually notifying all the simulation results, the proposed method RFO-MNN produced better quality of filtered images

Conclusion

This paper has concentrated on ultrasound images more explicitly, on the concealment techniques for the multiplicative noise. This work has contrasted with various denoising techniques used to suppress the SN in medicinal images acquired through ultrasound images. BF based RFO-MNN filtering method has been utilized to suppress the SN in US images. The simulation outcomes demonstrate that the BF based RFO-MNN filtering method performs better for the multiplicative noise concealment in US images. The better quality of denoised images is observed by using BF based RFO-MNN over other methods such that DTCWT-IBTV, BF and ANN. The proposed method BF based RFO-MNN produced better quality of de-speckled images with the PSNR of 34.89, SSIM of 0.89 and EPI of 0.67 values for US images.

References

- Ahmed, M. N., Yamany, S. M., Mohamed, N., Farag, A. A., & Moriarty, T. (2002). A modified fuzzy c-means algorithm for bias field estimation and segmentation of MRI data. *IEEE Transactions on Medical Imaging*, 21(3), 193-199
- Cheng, & Shi, X. (2004). A simple and effective histogram equalization approach to image enhancement. *Digital signal processing*, 14(2), 158-170.
- Madan Lal, Lakhwinder Kaur, Savita Gupta, 2016, 'Speckle Reduction with Edge Preservation in B-Scan Breast Ultrasound Images', *International Journal of Image, Graphics and Signal Processing*, vol. 9, pp.60-68.
- Gonzalez, R. C., Woods, R. E., & Eddins, S. L. (2004). *Intensity Transformations and Spatial Filtering Digital Image Processing Using MATLAB* (pp. 65-107): Pearson Prentice-Hall.
- Khan, Fick, D., Keogh, A., Crawford, J., Brammar, T., & Parker, M. (2005). Treatment of Acute Achilles Tendon Ruptures. A Meta-Analysis of Randomized, Controlled Trials. *The Journal of Bone Joint Surgery*, 87(10), 2202-2210. doi:10.2106/JBJS.D.03049
- Koli, M., & Balaji, S. (2013). Literature Survey on Impulse Noise Reduction. *Signal & Image Processing*, 4(5), 75-95. doi:10.5121/sipij.2013.4506.
- Loizou, C. P., & Pattichis, C. S. (2008). *Despeckle Filtering Algorithms and Software for Ultrasound Imaging*. *Synthesis Lectures on Algorithms and Software in Engineering*, 1(1), 1-166.
- Thivakaran, T. K., & Chandrasekaran, R. (2010). Nonlinear Filter Based Image Denoising Using AMF Approach. *International Journal of Computer Science and Information Security*, 7(2), 224-227.
- Achim, A., Bezerianos, A., & Tsakalides, P. (2001). Novel Bayesian Multiscale Method for Speckle Removal in Medical Ultrasound Images. *IEEE Transactions on Medical Imaging*, 20(8), 772-783.
- Kumar, G., & Bhatia, P. K. (2014). A Detailed Review of Feature Extraction in Image Processing Systems. Paper presented at the Fourth Intranational Conference on Advanced Computing & Communication Technologies.
- Khoury, V., Guillin, R., Dhanju, J., & Cardinal, É. (2007). Ultrasound of ankle and foot: overuse and sports injuries. Paper presented at the Seminars in musculoskeletal radiology.
- Sifuzzaman, M., Islam, M. R., & Ali, M. Z. (2009). Application of Wavelet Transform and its Advantages Compared to Fourier Transform. *Journal of Physical Sciences*, 13.



- Motwani, M. C., Gadiya, M. C., & Motwani, R. C. (2004, 109). Survey of Image Denoising Techniques. Paper presented at the Proc. of GSPx 2004, Santa Clara Convention Center, Santa Clara, CA.
- Singh, S., & Al-Mansoori, R. (2000). Identification of regions of interest in digital mammograms. *Journal of Intelligent Systems*, 10(2), 183-217.
- Kalavathi.P, Abinaya.M and Boopathiraja.S, 2017, 'Removal of Speckle Noise in Ultrasound Images using Spatial Filters', *Computational Methods, Communication Techniques and Informatics*, pp.174-177.
- Palwinder Singh, Leena Jai, 2013, 'Noise reduction in Ultrasound images using Wavelet and Spatial filtering Techniques', *IEEE 2nd International Conference on Information Management in the Knowledge Economy*, pp.57-63.
- Gagnon.L, Jouan.A, 1997, 'Speckle filtering of SAR images: A comparative study between complex-wavelet based and standard filters', *In SPIE Proc.*, 3169, pp. 80-91.
- Ranjitha M, 2016, 'Extraction and Dimensionality Reduction of Features for Renal Calculi Detection and Artifact Differentiation from Segmented Ultrasound Kidney Images', *IEEE International Conference on Computing for Sustainable Global Development*, pp.3087-3092.
- Dong, G., & Xie, M. (2005). Color clustering and learning for image segmentation based on neural networks. *IEEE transactions on neural networks*, 16(4), 925-936.
- Lui, S., Wei, J., Feng, B., Lu, W., Denby, B., Fang, Q., & Dang, J. (2012). An Anisotropic Diffusion Filter for Reducing Speckle Noise of Ultrasound Images Based on Separability. *Signal & Information Processing Association Annual Summit and Conference*.

